Supplement Materials

Supplement Material and Method

Immunoflorescent staining (IF staining)

Primary MEF cells transduced with or without GFP-NPGPx were seeded on cover slips to 50% confluence. Attached cells were washed with cold PBS, and fixed with 4% paraformaldehyde for 10 min at room temperature. Cells were further permeabilized with 1× PBS and 0.2% Triton X-100 at room temperature for 15 min, and stained with primary anti-GRP78 antibody and secondary anti-goat PE-conjugated antibody. Cells were stained with DAPI and mounted in Malino mounting buffer for visualization by fluorescent microscopy

GRP78 expression constructs

To generate human GRP78 (hGRP78) expression constructs, WT GRP78, hGRP78^{C41A}, hGRP78^{C420A}, and hGRP78^{C2A2} were subcloned from bacteria expression vector pET48 to mammalian expression plasmid pcDNA3.1-hygro (BamHI-GRP78-XhoI). These mammalian expression constructs were introduced into MEFs to perform reporter assay and IP experiment.

Preparation of GRP78 reconstituted MEFs

To generate hGRP78 proficient MEFs, mouse endogenous GRP78 (mGRP78) was knockdowned using shRNA targeting to 3'UTR of mGRP78 (shRNA was derived from RNAi core, Academia Sinica) and hGRP78 expression constructs were subsequently transfected into these MEFs. We use shEmpty (shRNA cloning vector) as knockdown control instead of shLuc to avoid non-targeting siRNA effect (Wei et al., 2011). GRP78

protein amount in these MEFs was shown in Supplement Figure 6, and these MEFs were ready for reporter assay or IP experiments.

Mass spectrometry analysis

After non-reducing SDS-PAGE analysis, the desired protein bands were cut and in-gel trypsin digestion was performed following standard procedure, and then subjected to mass spectrometry analysis. Nano-LC-MS/MS experiments were performed on a linear trap quadrupole-Fourier transform ion cyclotron resonance (LTQ-FT-ICR) mass spectrometer (Thermo Scientific) equipped with a nano-electrospray ion source (New Objective, Inc.) in positive ion mode. The liquid chromatography system consisted of an Agilent 1100 Series binary high-performance liquid chromatography pump (Agilent Technologies) with a Famos autosampler (LC Packings). The procedures and data analysis were performed as described (Xu and Freitas, 2009; Xu et al., 2010) . Briefly, the enzyme-digested protein samples were injected onto a self-packed precolumn (150 μm I.D. x 20 mm, 5 μm, 200 Å). Chromatographic separation was performed on a self-packed reversed-phase C18 nano-column (75 μm I.D. × 300 mm, 5 μm, 100 Å) by using 0.1 % formic acid in water (mobile phase A) and 0.1 % formic acid in 80 % acetonitrile (mobile phase B). A linear gradient was applied from 5 to 45 % mobile phase B for 40 min at a flow rate of 300 nL/min. Electrospray voltage was applied at 2 kV, and capillary temperature was set at 200°C. A scan cycle was initiated with a full-scan survey MS spectrum (*m*/*z* 300-2,000) performed on a FT-ICR mass spectrometer with a resolution of 100,000 at 400 Da. The ten most abundant ions detected in this scan were subjected to a MS/MS experiment performed in the LTQ mass spectrometer. Ion accumulation (Auto Gain Control target number) and maximum ion accumulation time for the full scan and MS/MS were set at 1×10^6 ions, 1,000 ms and 5×10^4 ions, 200 ms, respectively. Ions were fragmented by use of collision-induced dissociation (CID) with

the normalized collision energy set to 35 %, activation Q set to 0.3 and an activation time of 30 ms. For data analysis, all MS/MS spectra were converted to the mxXML format from the RAW file format by *MM File Conversion Tools*; the database search was then carried out by *MassMatrix* (http://www.massmatrix.net). A custom protein database containing P11021 (GRP78_HUMAN) and Q96SL4 (GPX7_HUMAN) was used for *MassMatrix*. The search parameters in *MassMatrix* included the following: 1) the custom enzyme digestion sites were on the C-terminal side of Arg, Lys, Phe, Leu, Trp, and Tyr; 2) the enzyme miss cleavage number was nine; 3) the error tolerance of precursor ions and the MS/MS fragment ions in the spectra were 10 ppm and 0.6 Da, respectively.

Supplemental table

Supplemental table 1. Primers used in Figure 7A

Gene		Sequence
Grp78	F	5'-CTGGGTACATTTGATCTGACTGG-3'
	R	5'-GCATCCTGGTGGCTTTCCAGCCATTC-3'
Xbp-1	F	5'-GAACCACAAACTCCAGCTAG-3'
	R	5'-GTCCATGGGAAGATGTTCTG-3'
Chop	F	5'- CGGCCTGGGAAGCAACGCAT-3'
	R	5'-ACCTCCCTGGTCAGGCGCTC-3'
Atf4	F	5'-ATGACCGAGATGAGCTTCCTG-3'
	R	5'- TGGAGAACCCATGAGGTTTCA-3'
Hprt	F	5′-ATGCCGACCCGCAGTCCCAGCGTCG-3′
	R	5′-TGACTGATCATTACAGTAGCTCTTC-3′

Supplemental figure legends

S. Figure 1. NPGPx has neither glutathione peroxidase activity nor thioredoxin peroxidase activity. GPX activity (A) and thioredoxin activity (B) assays. 2.5 μg and 5 μg of NPGPx or GPX1 were used in this assay. V0: the reduction rate of NADPH (measured by 340 nm absorbance). Peroxidase activity was determined by NADPH consumption. Glutathione and thioredoxin were used as substrate along with either glutathione reductase (A) or thioredoxin reductase (B) in reaction buffer containing Tris-HCl (100 mM, pH = 8) and NADPH (0.3 mM). NADPH consumption was measured by 340 nm absorbance.

S. Figure 2. NPGPx-covalent interacting complex is inducible by oxidative stress. Cell lysate derived from H_2O_2 treated/untreated human lung fibroblast WI38 or NPGPx-proficient osteosarcoma cell U2OS were subjected to Western blot analysis. NPGPx-interacting proteins were detected using NPGPx Ab.

S. Figure 3. Oxidized NPGPx contains reversible intramolecular disulfide bond. (A) Redox state of NPGPx *in vitro*. Purified NPGPx recombinant protein was treated with H_2O_2 (1 to 10 mM). The treatment converted NPGPx from reduced form (Red) to oxidized form (Ox) (left panel). Right panel: DTT (1 to 4 mM) reduced oxidized NPGPx (Ox). UT, untreated. (B) Redox states of NPGPx *in vivo*. Exogenously expressed NPGPx in U2OS cells has two forms (Red and Ox). Treatment of cells with H_2O_2 converted NPGPx from reduced form (Red) to an oxidized form (Ox) (left panel); both of the oxidized forms became as reduced form by treatment of lysates with DTT (100 mM).

S. Figure 4. Schematics of human GRP78. Human GRP78 encodes 654 amino acids

and contains several functional domains: (1) ER signaling peptide (1-18 amino acid), (2) ATPase domain (125-280 amino acid), (3) peptide-binding domain (400-500 amino acid), and (4) KDEL (651-654 amino acid) which retains GRP78 in ER. Cys41 and Cys420 are located in different domains of GRP78.

S. Figure 5, NPGP-GRP78 interaction is released after 4 hour H_2O_2 treatment. Reciprocal IP of NPGPx and GRP78 in lysates prepared using WT MEFs treated with H_2O_2 for the indicated duration. Precipitated proteins were subjected to Western blot analysis. After 30 minutes of H_2O_2 treatment, NPGPx-GRP78 interaction declined and then released after 4 hours of treatment.

S. Figure 6. Cys41 and Cys420 are required for GRP78 full activation in facilitating folding *in vivo*. (A) Protein expression level in cells proficient with WT GRP78, hGRP78^{C41A}, hGRP78^{C420A}, and hGRP78^{C2A2}as described in Supplement Material and Method. Each mutants represented comparable protein level to WT GRP78, suggesting Cys to Ala substitution did not interfere GRP78 protein stability. (B) *In vivo* chaperon activity assay. Luciferase expressing WT MEFs reconstituted with or without hGRP78 were used in this assay. Cells were incubated at 42 ^{o}C for 30 minutes followed by recovery for 1 hour (HS-R1hr) or 2 hours (HS-R2hr) in 37 ^{o}C incubator. Cell harvested from indicated time points were subjected to Luciferase activity assay. It is noted that Luciferase activity was not recovered in hGRP78^{C41A} or hGRP78^{C420A} expressing cells, suggesting loss of either one of Cys residue compromised GRP78 chaperone activity. Control: cells without 42 ^{o}C heat-shock.

S. Figure 7, **NPGPx inactivation accelerated aggresome formation in misfolded protein GFP-250 expressing MEFs and increased cell death.** (A) Aggresome in

wild-type or NPGPx$^{-/-}$ MEFs. GFP-250, a cytosolic chimera protein, was transduced into wild-type or NPGPx$^{-/-}$ MEFs. Aggresomes (green dots) were visualized using fluorescent microscopy after 1 hour treatment of proteosome inhibitor MG132 (10 μg/ml). (B) Kinetics of aggresome formation. NPGPx cells transduced with GFP-250 were treated with MG-132 (10 μg/ml) for 1 to 4 hours. Aggresome in WT or NPGPx$^{-/-}$ MEFs were visualized by fluorescent microscopy. 10 individual fields were recorded every hour, and kinetics of aggresome formation was determined by plotting the percentage of aggresome-containing MEFs. (C) Time-lapse of GFP-250 expressing MEFs. MEFs expressing GFP-250 were seeded in culture dishes and recorded by time-lapse florescent microscopy. After 15 hours, the aggresome containing cell WT were alive while the NPGPx$^{-/-}$ MEFs dead. (D,E) Annexin V staining. MEFs stained with Annexin V and PI were analyzed by FACS sorter. The percentage of apoptotic cells from total MEFs (D) or GFP^{+} MEFs (E) was shown.

S. Figure 8, **GFP-250 expressing MEFs reconstituted with hGRP78^{C2A2} contain more aggresome compare to cells expressed WT hGRP78.** (A) Aggresome in WT GRP78 or hGRP78^{C2A2} reconstituted MEFs transduced with GFP-250. Aggresomes (green dots) were visualized using fluorescent microscopy. (B) Percentage of cells contained aggresome. Pictures from 4 individual fields were taken, and the ratio of aggresome-containing cells was determined.

S. Figure 9. Mass spectrum analysis of NPGPx intramolecular disulfide bond. (A, B) MS2 spectrum of the disulfide bond cross-linked peptide between NPGPx Cys57 (A) and Cys86 (B). (C) Schematics of NPGPx intramolecular Cys-S-S-Cys sequences. NPGPx Cys57-S-S-Cys86 was shown.

S. Figure 10. Illustration (using swiss pdbviewer) of the intramolecular disulfide bond of NPGPx. NPGPx (without 1-18 signal peptide) crystal structure in PDB (ID: 2p31) was shown. Cys40 and Cys69 in this figure correspond to Cys57 and Cys86, respectively, of NPGPx. As it is shown, Cys40 is located at a turn between α-helix and β-sheet, and Cys69 is located at another β-strand. The distance between these two Cys residues in the reduced NPGPx crystal was 11.58 Angstrom.

S. Figure 11. Mass Spectral analysis of NPGPx-GRP78 complex. (A, B) MS2 spectra of the disulfide bond cross-linked peptide between NPGPx Cys86 (A) and GRP78 Cys41 (B). (C, D) MS2 spectra of the disulfide bond cross-linked peptide between NPGPx Cys86 (C) and GRP78 Cys420 (D).

S. Figure 12. Oxidized GRP78 contains Cys41-Cys420 intramolecular disulfide bond. (A, B) MS2 spectral analysis showing the Cys-S-S-Cys bonding between Cys41 and Cys420 of GRP78. GRP78 monomer from SDS-PAGE was purified and digested as described in Supplemental Material and Method. Peptides containing Cys41 (A) or Cys420 (B) with Cys covalent interactions are shown. The ratio of Cys41-S-S-Cys420 containing GRP78 in rGRP78 to lane 3 in Figure 6 is roughly 1:40. (C) Non-reducing SDS-PAGE of WT GRP78 and hGRP78C2A2. Recombinant 6xHis-GRP78 proteins were purified, treated with H_2O_2 or TCEP with indicated concentration and separated in SDS-PAGE. Bands 1, 2 and 3 were analyzed by mass spectrum as described in (A).

S. Figure 13. Quantity of GRP78 interacting luciferase in Figure 6E. Luciferase protein amount from each indicated condition from Western blot of Figure 6C and the other two independent experiments was quantified by using UVP image system. The * indicates p value smaller than 0.005.

S. Figure 14. Kidney antibody deposition and anti-nuclear antibody were observed in NPGPx deficient mice. (A) Kidney frozen section derived from WT or NPGPx$^{-/-}$ moribund mice were subjected to electron microscopy. Region D: antibody deposition. (B) Immunofluorescent staining using serum (1:500 dilution) from WT or NPGPx$^{-/-}$ mice to against WT MEF cells. FITC-conjugated secondary antibody was used to visualize autoantibodies. Green: mouse serum autoreactive IgG; blue: DAPI. It revealed that serum from 10 month old NPGPx$^{-/-}$ mice contained anti-nuclear antibody.

References

Wei, P.C., Lo, W.T., Su, M.I., Shew, J.Y., and Lee, W.H. (2011). Non-targeting siRNA induces NPGPx expression to cooperate with exoribonuclease XRN2 for releasing the stress. Nucleic Acids Res *40*, 323-332.

Xu, H., and Freitas, M.A. (2009). MassMatrix: a database search program for rapid characterization of proteins and peptides from tandem mass spectrometry data. Proteomics *9*, 1548-1555.

Xu, H., Hsu, P.H., Zhang, L., Tsai, M.D., and Freitas, M.A. (2010). Database search algorithm for identification of intact cross-links in proteins and peptides using tandem mass spectrometry. J Proteome Res *9*, 3384-3393.

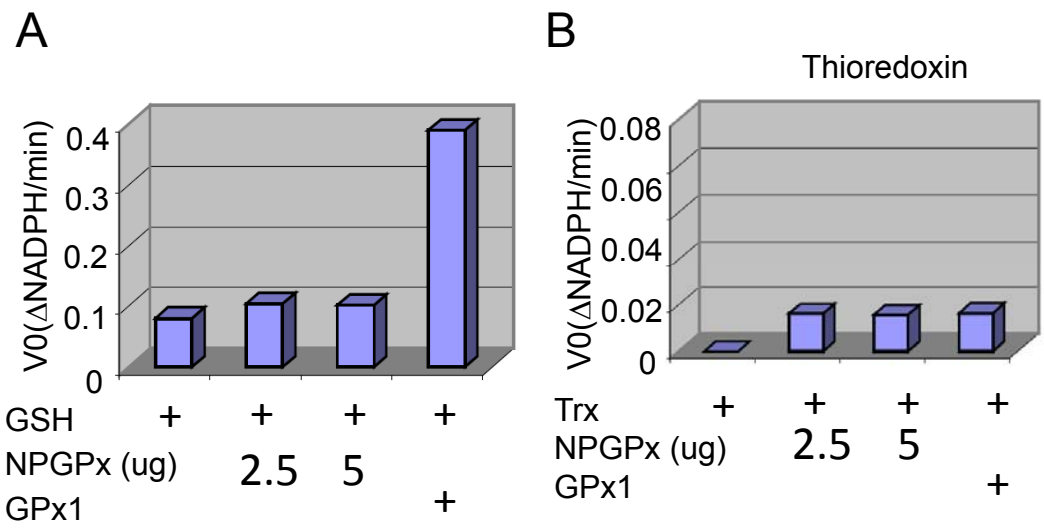

S. Figure 1, Wei *et. al.*

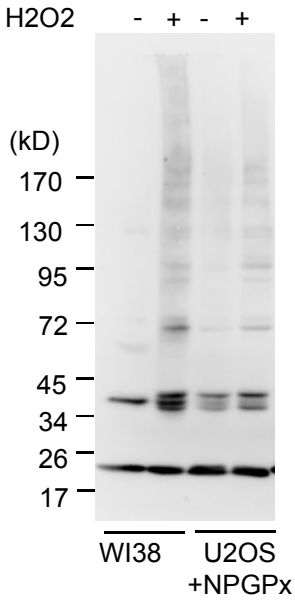

S. Figure 2, Wei *et. al.*

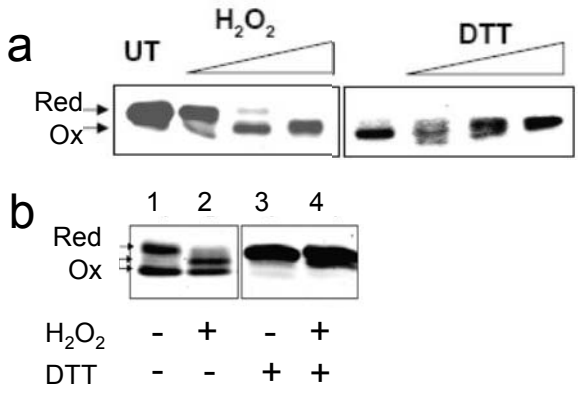

S. Figure 3, Wei *et. al.*

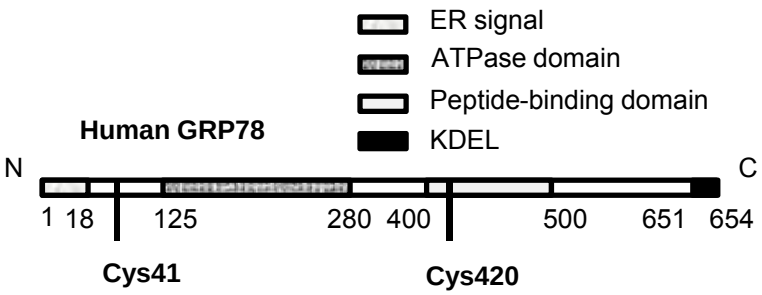

S. Figure 4, Wei *et. al.*

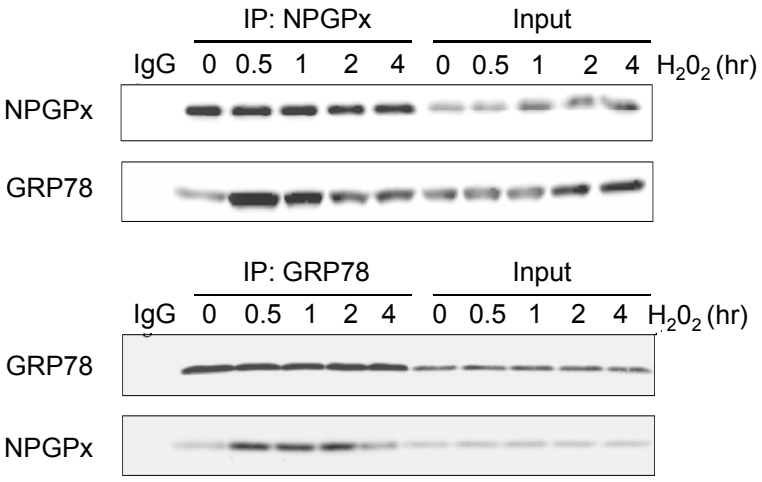

S. Figure 5, Wei *et. al.*

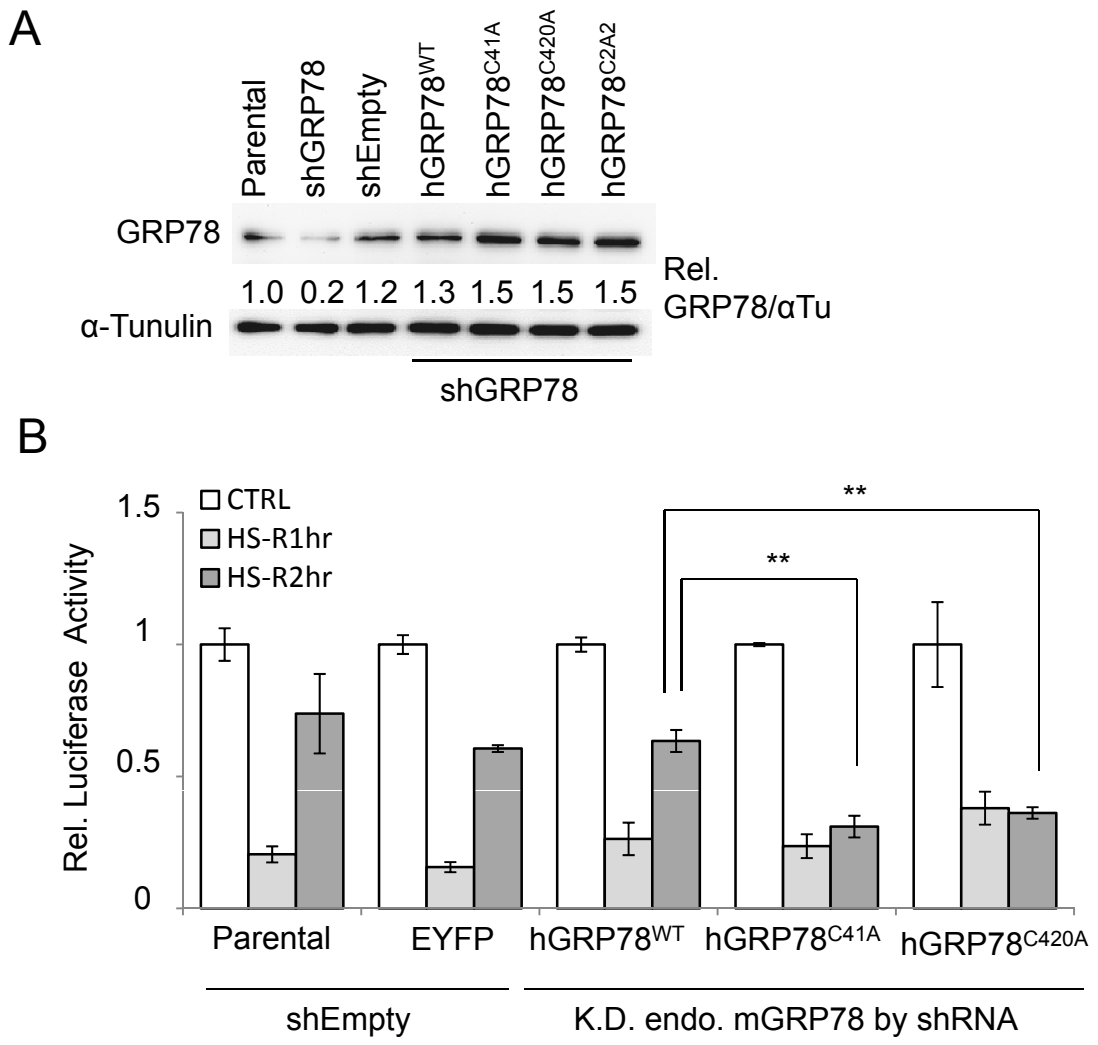

S. Figure 6, Wei *et. al.*

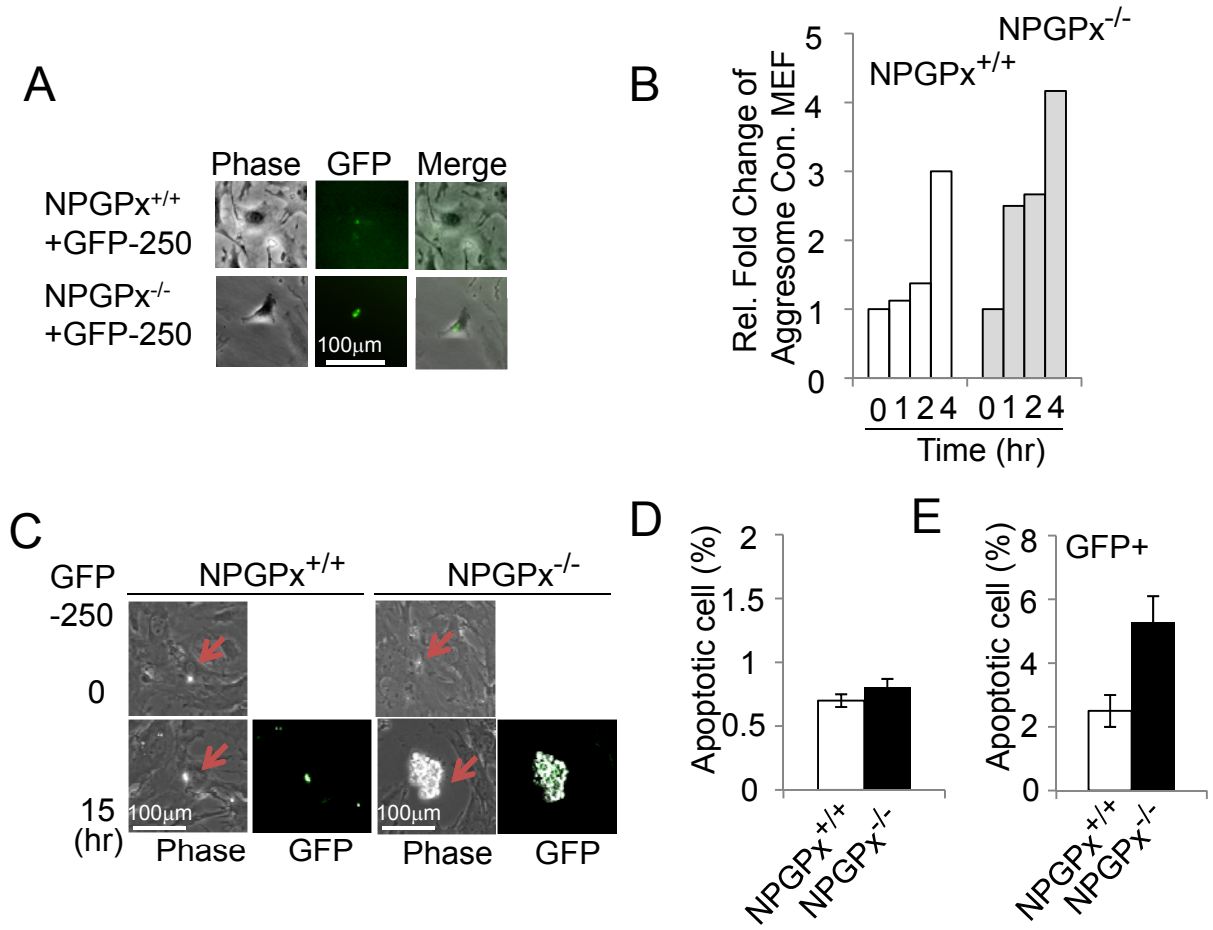

S. Figure 7, Wei *et. al.*

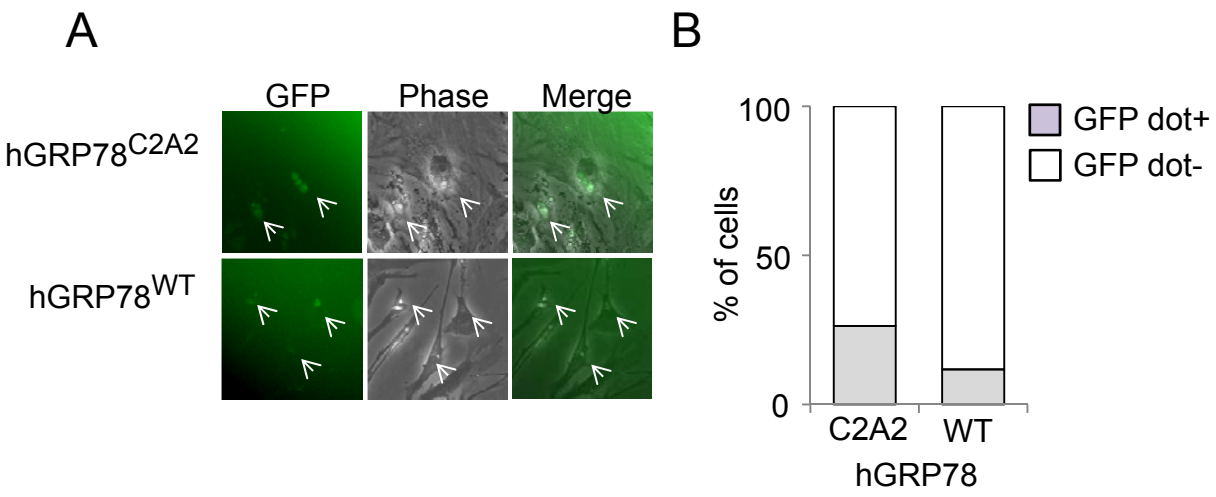

S. Figure 8, Wei *et. al.*

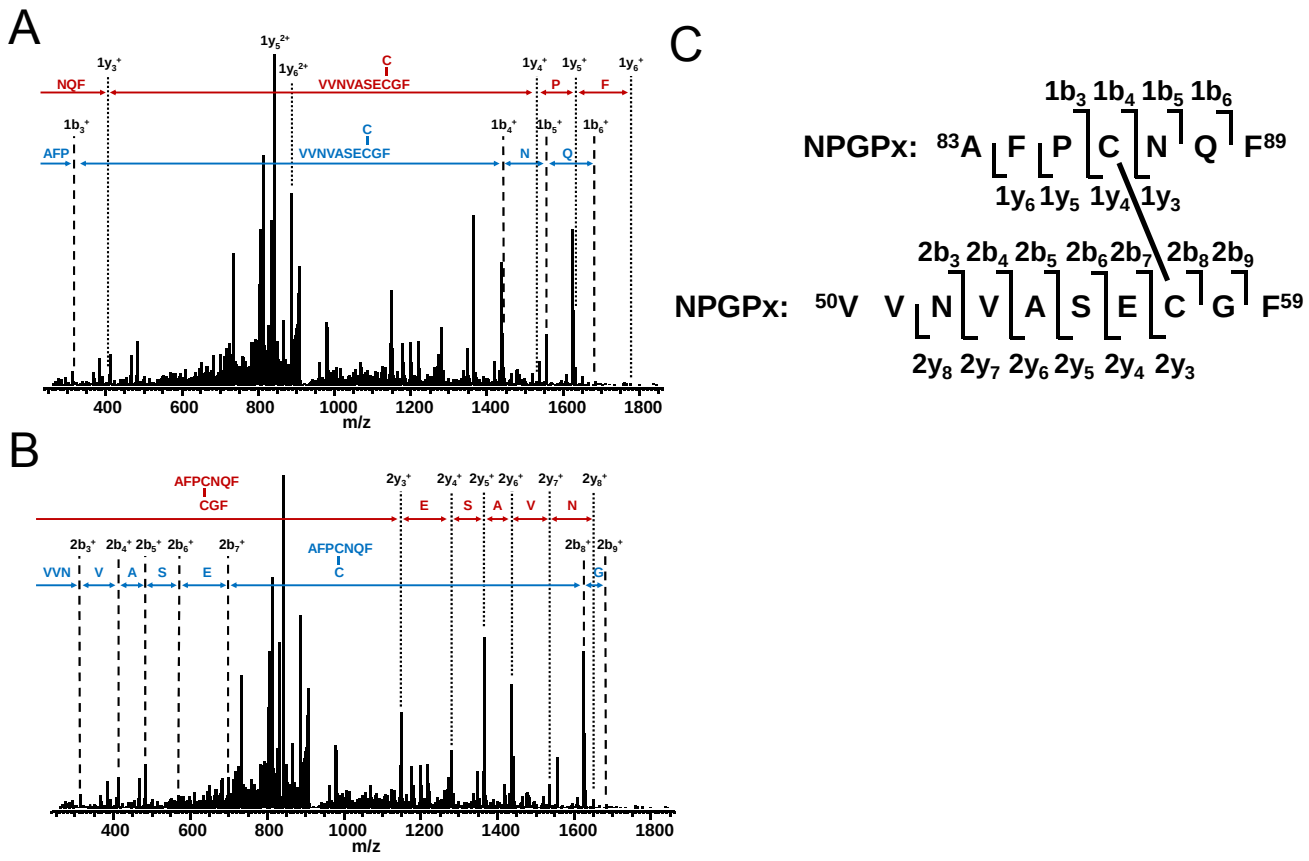

S. Figure 9, Wei *et. al.*

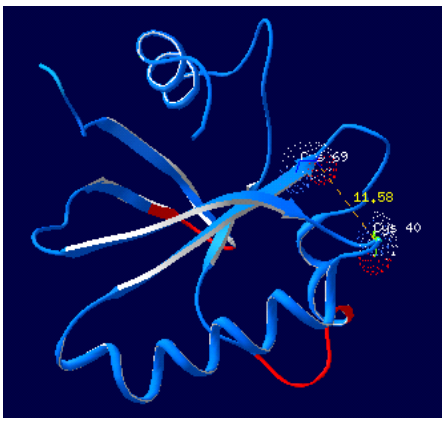

S. Figure 10, Wei *et. al.*

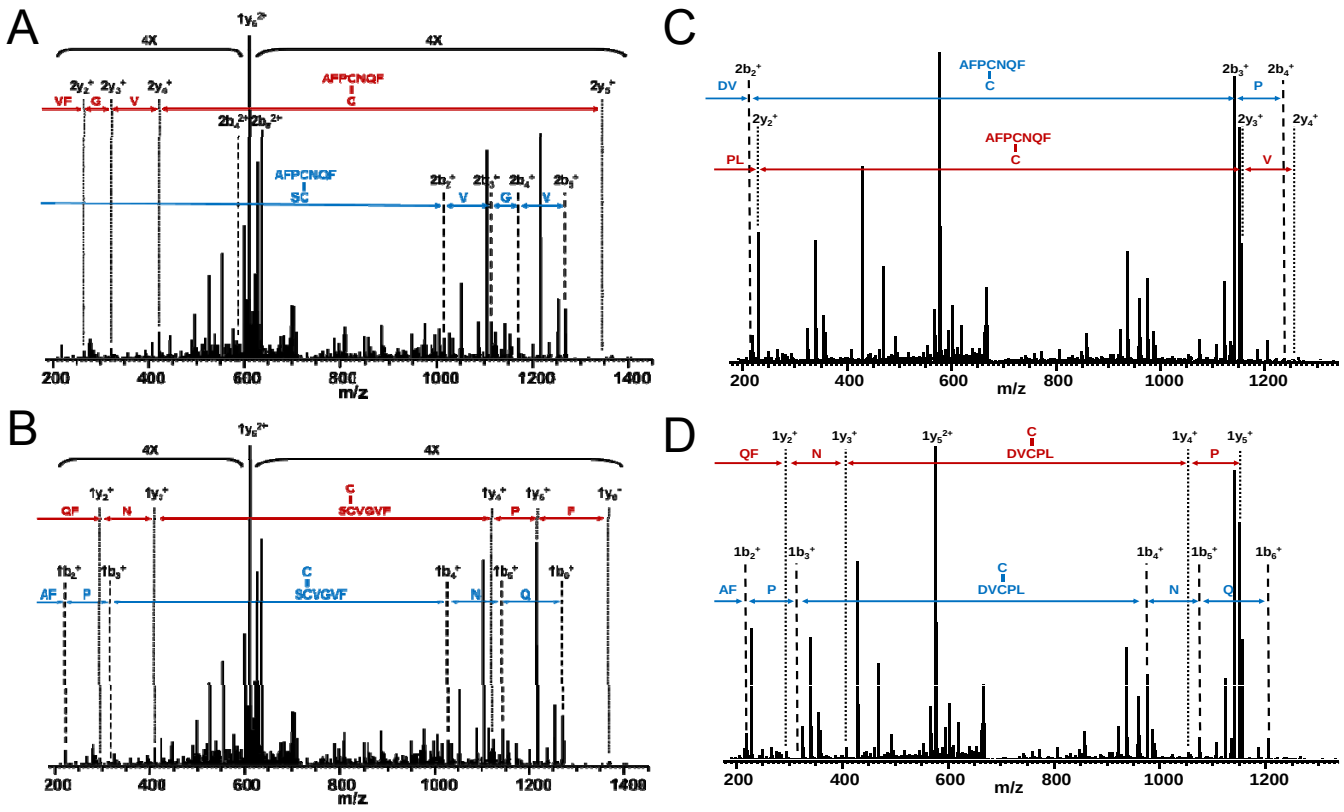

S. Figure 11, Wei *et. al.*

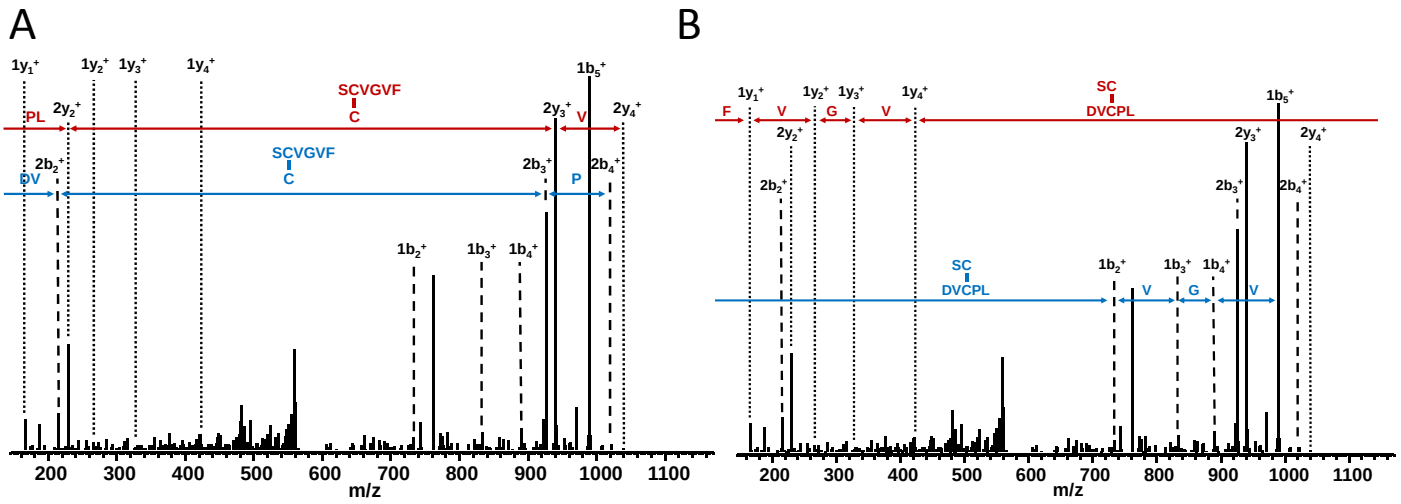

C

GRP78^{C2A2}			+	+		+		+
GRP78^{WT}	+	+			+		+	
TCEP 10mM							+	+
H_2O_2 9mM		+		+	+	+		

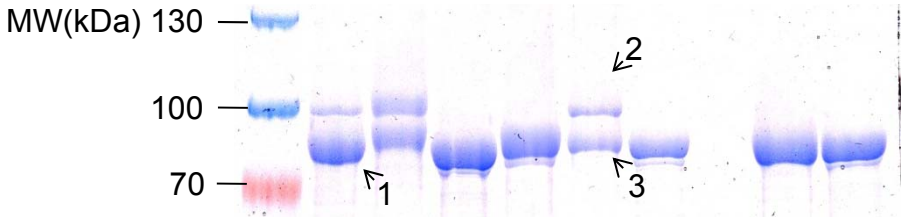

1: GRP78, no Cys41-Cys420,;no SO_3H
2: GRP78 Cys41-Cys420
3: GRP78 Cys41-SO_3H

S. Figure 12, Wei *et. al.*

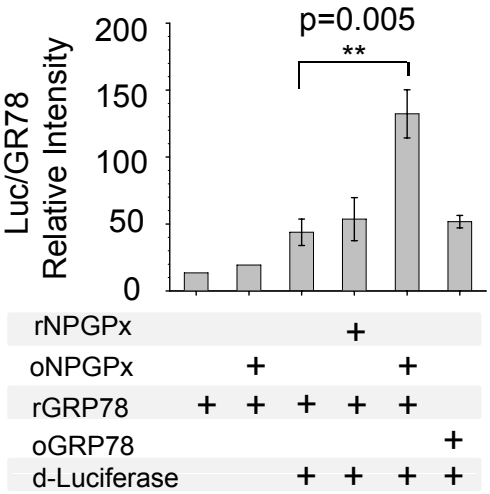

S. Figure 13, Wei *et. al.*

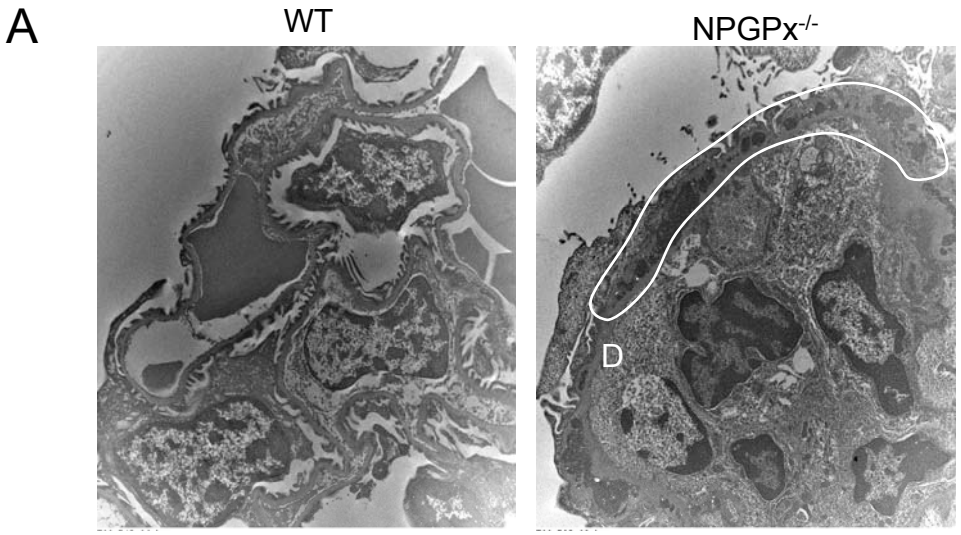

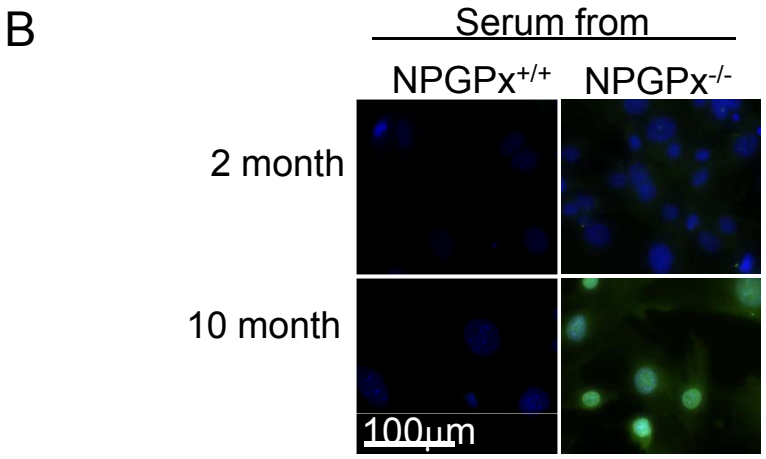

S. Figure 14, Wei *et. al.*